MOUNTAIN-PLAINS CONSORTIUM

MPC 25-579 | M. Elnahla, Y. Guo and R. Atadero

ADDRESSING THE FEASIBILITY OF EMPLOYING NDE DATA FOR BRIDGE CONDITION ASSESSMENT USING GAUSSIAN PROCESS REGRESSION

A University Transportation Center sponsored by the U.S. Department of Transportation serving the Mountain-Plains Region. Consortium members:

Colorado State University
North Dakota State University
South Dakota State University
University of Colorado Denver
University of Denver
University of Utah
Utah State University
University of Wyoming

Technical Report Documentation Page

1. Report No.	2. Government Accession No.	3. Recipient's Catalog No.
MPC-618		

4. Title and Subtitle	5. Report Date / 6. Performing Organization Code
Addressing the Feasibility of Employing NDE Data for Bridge Condition Assessment Using Gaussian Process Regression	5. Report Date: October 2025 6. Performing Organization Code:
7. Author(s) Mahmoud Elnahla https://orcid.org/0009-0003-7875-2747 Yanlin Guo https://orcid.org/0000-0002-7162-6508 Rebecca Atadero https://orcid.org/0000-0002-7477-1620	8. Performing Organization Report No. MPC 25-579
9. Performing Organization Name and Address Colorado State University 711 Oval Drive Fort Collins, CO 80521	10. Work Unit No. (TRAIS) 11. Contract or Grant No. 69A3551747108
12. Sponsoring Agency Name and Address Mountain-Plains Consortium North Dakota State University PO Box 6050, Fargo, ND 58108	13. Type of Report and Period Covered Final Report 14. Sponsoring Agency Code

15. Supplementary Notes

Supported by a grant from the US DOT, University Transportation Centers Program

16. Abstract

Existing bridge deterioration models rely on subjective national bridge inventory (NBI) condition ratings from visual inspections, which lack the objective assessments needed for informed repair and maintenance decisions. Non-destructive evaluation (NDE) tests, such as impact echo (IE), provide quantitative and objective condition evaluation data. However, these data have been underutilized for deterioration modeling due to data scarcity (one to three records per bridge). This report introduces a novel concept to put limited NDE data to more valuable use. Specifically, a Gaussian process regression (GPR) model is developed using IE records from the Long-Term Bridge Performance (LTBP) database. The GPR model offers two key advantages: it accurately predicts delamination for untested bridges (i.e., the bridges without IE records) with characteristics similar to those in the training data, and identifies bridges with high prediction uncertainty, enabling them to be prioritized for NDE testing to improve the model's future delamination predictions. This approach enhances NDE inspection planning and resource allocation by focusing on the most uncertain structures for testing. Moving forward, the report identifies challenges and opportunities in the LTBP database, urging changes in current NDE data collection practices to support more strategic NDE applications, data reuse, and accurate deterioration modeling.

17. Key Word	18. Distribution Statement
asset management, bridges, condition surveys, data analysis, evaluation, infrastructure, life cycle costing	Public distribution

19. Security Classif. (of this report)	20. Security Classif. (of this page)	21. No. of Pages	22. Price
Unclassified	Unclassified	33	n/a

Form DOT F 1700.7 (8-72) Reproduction of completed page authorized

Addressing the Feasibility of Employing NDE Data for Bridge Condition Assessment Using Gaussian Process Regression

Mahmoud Elnahla
Ph.D. student
Colorado State University
Department of Civil and Environmental Engineering
Fort Collins, Colorado, 80523-1372
M.elnahla@colostate.edu

Yanlin Guo
Associate Professor
Colorado State University
Department of Civil and Environmental Engineering
Fort Collins, Colorado, 80523-1372
yanlin.guo@colostate.edu

Rebecca A. Atadero
Professor
Colorado State University
Department of Civil and Environmental Engineering
Fort Collins, Colorado, 80523-1372
Rebecca.atadero@colostate.edu

October 2025

Acknowledgment

The authors extend their gratitude to the Mountain Plains Consortium, the U.S. Department of Transportation, the Research and Innovative Technology Administration, and Colorado State University for funding this research.

Disclaimer

The contents of this report reflect the views of the authors, who are responsible for the facts and the accuracy of the information presented. This document is disseminated under the sponsorship of the Department of Transportation, University Transportation Centers Program, in the interest of information exchange. The U.S. Government assumes no liability for the contents or use thereof.

North Dakota State University does not discriminate in its programs and activities on the basis of age, color, gender expression/identity, genetic information, marital status, national origin, participation in lawful off-campus activity, physical or mental disability, pregnancy, public assistance status, race, religion, sex, sexual orientation, spousal relationship to current employee, or veteran status, as applicable. Direct inquiries to Vice Provost, Title IX/ADA Coordinator, Old Main 100, (701) 231-7708, ndsu.eoaa@ndsu.edu.

ABSTRACT

Existing bridge deterioration models rely on subjective national bridge inventory (NBI) condition ratings from visual inspections, which lack the objective assessments needed for informed repair and maintenance decisions. Non-destructive evaluation (NDE) tests, such as impact echo (IE), provide quantitative and objective condition evaluation data. However, these data have been underutilized for deterioration modeling due to data scarcity (one to three records per bridge). This report introduces a novel concept to put limited NDE data to more valuable use. Specifically, a Gaussian process regression (GPR) model is developed using IE records from the Long-Term Bridge Performance (LTBP) database. The GPR model offers two key advantages: it accurately predicts delamination for untested bridges (i.e., the bridges without IE records) with characteristics similar to those in the training data, and identifies bridges with high prediction uncertainty, enabling them to be prioritized for NDE testing to improve the model's future delamination predictions. This approach enhances NDE inspection planning and resource allocation by focusing on the most uncertain structures for testing. Moving forward, the report identifies challenges and opportunities in the LTBP database, urging changes in current NDE data collection practices to support more strategic NDE applications, data reuse, and accurate deterioration modeling.

TABLE OF CONTENTS

LIST OF TABLES

LIST OF FIGURES

EXECUTIVE SUMMARY

This report introduces a novel method for utilizing limited NDE data from various bridge decks to predict the deterioration of other decks. Traditional deterioration models often predict the National Bridge Inventory (NBI) condition rating, which is subjective and qualitative, limiting its direct application in bridge management and maintenance decisions. To overcome these challenges, a Gaussian Process Regression (GPR) model was developed based on Impact Echo (IE) data to predict bridge deck delamination. Due to the limited availability of NDE records (38 in total), careful data selection, filtration, and processing were implemented. This process yielded 20 IE records that were used in the model development. Bayesian optimization was used to find the optimum GPR hyperparameters where 18 points were used for training and 2 points were left for testing. The proposed model achieved an average root mean square error (RMSE) of 11.45% for cross-validation data and 10.70% for testing data. Given that the GPR model provides a prediction with an uncertainty prediction, it is used to construct an NDE inspection planning framework. Moving forward, the limitations within the NDE data available in the LTBP database have been identified, along with recommendations for improved data collection practices to optimize the leveraging of the existing NDE data.

1. INTRODUCTION

Bridges are one of the most important infrastructures for any country and maintaining bridge condition is an important task. In 2023, among 621,581 U.S. bridges, 48.9% were reported in fair condition, while 6.8% were in structurally deficient or poor condition, requiring $47 billion for rehabilitation according to Federal Highway Administration data (FHWA, 2023). Bridge decks are the most damaged component within a bridge (Morcous et al., 2010) since they are directly subjected to traffic loads and severe environmental conditions, especially in cold regions where deicing chemicals are used (Kim & Yoon, 2009). Figure 1.1 illustrates the historical performance of bridge decks across the United States. The figure shows a decline in the percentage of bridge decks in "Good" condition, with a steady increase in the "Fair" condition over the past three decades. Although the "Poor" condition remains low, a slight increase in the last four years signals emerging concerns (FHWA, 2024). These trends suggest aging infrastructure and highlight the need to better understand and model bridge deterioration for more effective maintenance strategies.

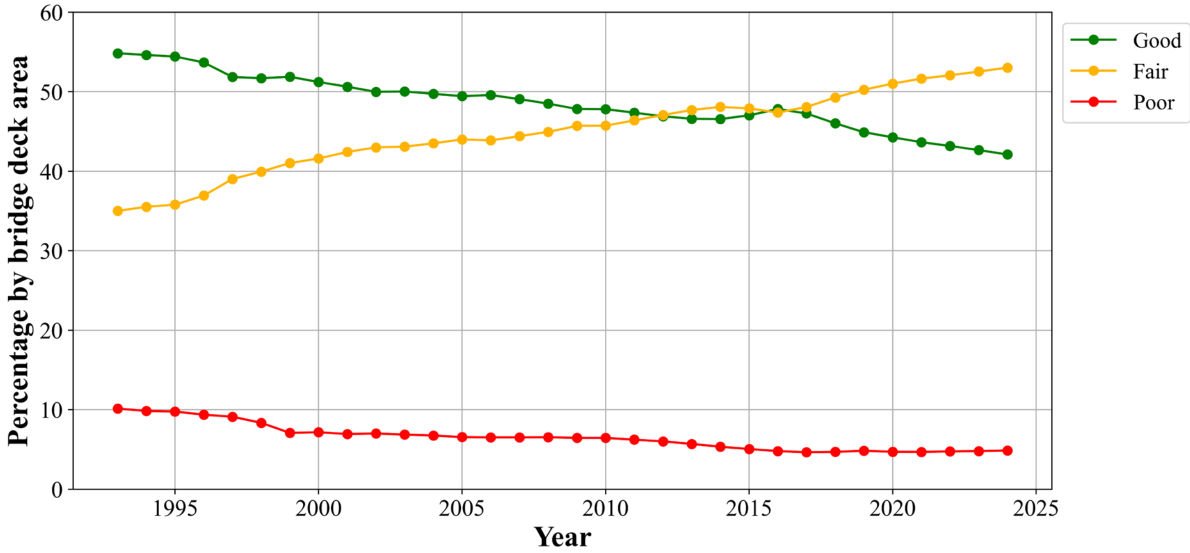

Figure 1.1 Time history of bridge deck area condition percentages ("Good," "Fair," and "Poor") based on the latest FHWA data (2024)

To gain a more comprehensive understanding of the deterioration process and develop effective maintenance plans, researchers have turned to the development of bridge deterioration models. Deterioration models are considered a primary component in any bridge management system (BMS). They have been extensively adopted by many BMSs such as BRIDGIT and AASHTOW, which are the most popular in the U.S. (Dinesh & Gongkang, 2009). Deterioration models provide information that helps allocate limited funds and resources to meet current needs and anticipate future conditions. Currently, deterioration models adopted by different state departments of transportation (DOTs) are used for long-range budget planning, project scoping and/or planning, and life cycle cost analysis (Caltrans Division of Research, 2020). Although deterioration models utilizing different inputs and outputs have been developed, models predicting National Bridge Inventory (NBI) condition ratings are the most common. This might be due to the relative simplicity, accessibility, and availability of NBI condition rating data. However, two main challenges restrict the utility of these models: the limitations of different modeling techniques and the final prediction output of these models.

First, the limitations of the employed modeling techniques stem from their inherent assumptions or the large amount of data required for training. Generally, deterioration models can be categorized into four main types: deterministic, stochastic, mechanistic, and artificial intelligence (AI) models. Deterministic models neglect the uncertainty and stochastic nature of infrastructure deterioration. Stochastic models, conversely, consider the probabilistic nature of bridge deterioration. However, stochastic state-based models suffer from being memoryless and time-homogenous (Srikanth & Arockiasamy, 2020); whereas stochastic time-based models are limited by the complexity of distribution parameter estimation and the extent of historical data required to provide appropriate results (Mauch & Madanat, 2001). Mechanistic models mainly yield efficient results when implemented at the project level, but they are less useful for an inventory of bridges (Nickless & Atadero, 2018). Recently developed AI-based models excel in handling the complex behavior of deterioration. Nonetheless, most AI models require a considerably large set of data to avoid fitting problems (Althaqafi & Chou, 2022; Huang, 2010; Nguyen & Dinh, 2019; Sobanjo, 1997; Tokdemir et al., 2000). A recently developed model, Gaussian process regression (GPR), effectively addresses the issue of data scarcity, making it a robust choice even with limited data. Dhada et al. (2020) employed the GPR model to predict the condition index of bridge elements for bridges in the UK. Since the GPR model is non-parametric, flexible, and robust, it is employed in this report.

Second, the final prediction output of the previously discussed models was generally the NBI condition rating. This rating has many limitations such as the subjectivity of visual inspection, no information about deterioration that cannot be detected by visual inspection, and insufficient information for some condition ratings, especially low ratings (Winn & Burgueño, 2013). Moreover, predicted condition ratings cannot be utilized effectively in predictive maintenance and decision-making. For example, many DOTs rely on a decision matrix for deterioration repairs where there is a specific maintenance measure corresponding to each range of deterioration percentage. Taking the Michigan Department of Transportation as an example, the selection of maintenance strategies varies with the extent of delamination. Low delamination percentages may warrant the application of epoxy overlays, while higher percentages necessitate shallow or deep patch repairs (MDOT, 2021). However, predicted condition ratings offer limited value to inform these decisions as they are abstract and do not provide the necessary quantitative assessment of deterioration.

To address NBI condition rating limitations, different non-destructive evaluation (NDE) techniques have been used in deterioration assessment. NDEs employ different advanced technologies to capture data quantifying the underlying bridge deterioration. Various instruments are used to scan the bridge, process the data based on physical theories, and finally provide a condition map that describes quantitatively the ongoing deterioration. Accordingly, they overcome the previously mentioned limitations of condition rating since they provide objective and relatively accurate quantitative assessment data. However, NDEs are costly, considering the direct costs of equipment, data analytics, and human resources, as well as indirect costs due to traffic closure (Taylor et al., 2017). NDE’s cost means that it has not been adopted as a routine inspection technique for all bridges, rather NDE is used on bridges with known deterioration to provide a more detailed assessment for maintenance planning.

Although NDEs offer a promising solution for bridge inspection, their output is typically limited to assessment of a single bridge, and there has been no effort to use the data for bridge deterioration modeling. The main reason NDE data are not being put to greater use is that there is no clear strategic plan for NDE data collection and sharing. Accordingly, the data are not collected on a fixed time basis and data collected by different companies are not publicly shared and not necessarily stored in the same format. However, resolving such limitations will help employ NDE data in deterioration modeling, extending their utility and making the collection of these data more cost-effective. NDE data collected strategically with well-designed spatial and temporal sampling plans will fulfill a broader goal where they can be efficiently utilized in deterioration modeling across different bridges within bridge networks and not just to assess one bridge’s current condition.

2. PURPOSE

This report proposes a novel concept for leveraging NDE data from different bridges to allow quantitative and objective prediction of bridge deck deterioration. To demonstrate this concept, a GPR model is developed based on IE records obtained from the Long-Term Bridge Performance (LTBP) database to model the concrete deck delamination of multi-girder bridges. Delamination occurs when part of the concrete surface debonds from the underlying base, a critical issue for bridge decks and the primary cause of most deck repairs (Gucunski et al., 2013). Delamination can result from short-term factors, such as premature finishing, or long-term issues like freeze-thaw cycles and corrosion (Concrete New Zealand Incorporated, 2021).

The proposed model will serve two purposes: First, the model will handle the complex behavior of bridge deterioration and the diversity of bridge parameters to predict an approximate percentage of delamination for bridges with no IE records. Second, the model provides prediction uncertainty estimation, which can be used to prioritize NDE scheduling, particularly for bridges with high prediction uncertainty. Both purposes support informed maintenance decisions and optimal resource allocation. A secondary purpose of this report is to highlight some of the limitations associated with NDE data that are available in the LTBP database and suggest ways to improve LTBP data collection that will help enhance bridge deterioration modeling.

3. NDE DATA AVAILABLE IN THE LTBP DATABASE

This report is based on the NDE data available in the LTBP database. The LTBP database offers massive data for almost 623,000 bridges throughout the U.S. However, only 38 bridges have NDE data, which will constitute the available dataset for this report. For these bridges, the database contains information about most of the bridge parameters, such as structural system, construction material, dimensions, traffic, environmental conditions, and NDE data. The NDE data contain records obtained from different non-destructive tests, including impact echo (IE), ground penetrating radar, electric resistivity, half-cell potential, and ultrasonic surface waves. The NDE test results are provided in two forms: raw data in the form of voltage-time signals and processed data in the form of condition maps. At the time of this report, most NDE data provided in the LTBP are only given for one to three years. These years are usually 2013, 2015, and 2017.

Although many of these NDEs provide deterioration data that could be used in the proposed model, this report will focus on predicting one type of deterioration, which is deck delamination. This prediction is achieved by using delamination percentages quantified from the available IE records. IE records are used because among all the different NDE tests available, IE is often considered the best NDE test for detecting delamination. More specifically, past studies showed that IE is capable of estimating deck thickness with an error of 3% (Sansalone and Streett, 1997). Also, previous research has utilized ground-coupled IE for detecting shallow delaminations in concrete structures (Azari et al., 2014; Olson et al., 2011; Sansalone & Carino, 1989). These studies showed the capability of identifying delaminations as small as 100 mm in diameter. Besides, IE is considered the primary NDE technique in the LTBP program for the detection and characterization of deck delamination (Gucunski et al., 2017). According to the second Strategic Highway Research Program (SHRP 2), IE is the best NDE method for the detection of delaminations when considering accuracy and reliability (Gucunski et al., 2012).

4. IMPACT ECHO BACKGROUND

An IE test is conducted by applying an impact force using a steel ball to the concrete surface producing a compression wave (P-wave) through the deck thickness. The wave undergoes multiple reflections when it hits the bottom of the deck or any subsurface defect. The reflected wave is recorded by an adjacent receiver. If the receiver is close to the impact point, the round-trip travel distance is $2T$, where T is the distance between the test surface and the reflection surface. Although it is possible to analyze the recorded signal in the time domain, a more straightforward and robust analysis is usually conducted in the frequency domain. Hence, the recorded time domain signal is then converted to the frequency domain using fast Fourier transform (FFT). This frequency is directly associated with the physical properties of the deck, where the wave travel time is calculated as twice the deck thickness divided by the P-wave velocity. Consequently, the P-wave frequency is the inverse of this time interval. The relationship between thickness resonance frequency (f_{th}), deck thickness (H), and P-wave velocity (v_p) is given by the approximate relationship:

$$f_{th} = \frac{\beta v_p}{2H} \tag{1}$$

where (v_p) typically ranges between 3,500 m/s to 4,500 m/s (Lee & Oh, 2016) and can either be measured or assumed, and (β) is a modification factor, which takes the value of approximately 0.96 for concrete plates.

Since there is no unified approach to interpret the IE signals, there are many criteria that can be followed to classify the resulting IE signal into two, three, or four classes representing the deck condition (Torlapati et al., 2023). Generally, for intact decks, emitted signals are reflected back and forth between the two free surfaces of the deck. Accordingly, the thickness resonance frequency stands out as the dominant peak. On the other hand, decks in serious condition will excite the flexural vibrational mode of the upper delaminated areas. In this case, the dominant peak frequencies will be much lower than the thickness resonance frequency, usually below 5 KHz. Finally, intermediate cases may be present and are identified by several dominant peaks caused by the initiation of shallow delaminations or the presence of deep delaminations. A widely adopted approach is to classify the IE data into four distinct classes: good, fair, poor, and serious. The classification results are then visualized as a color-coded condition map for easier data interpretation (Gucunski et al., 2008a).

5. DATA SELECTION AND FILTRATION

The GPR model is data-driven. Thus, careful data preparation is required to ensure quality of the input data and, consequently, the model. First, among different main span design systems in the LTBP database, including box, truss, and stringer/multi-beam, bridges with stringer/multi-beam systems are selected for modeling. This choice is made because stringer/multi-beam bridges are the most common type with available IE records. Out of the 38 bridges with IE records, 34 bridges have a stringer/multi-beam system. Another reason is that they are generally the most stressed and high-maintenance types of highway structures (Morcous & Lounis, 2007). Second, bridges with known deck information such as thickness data are selected because deck information will be used in both data processing and modeling steps. Out of 34 bridges, only 26 meet this requirement and are included in the analysis.

The selected 26 bridges are then filtered in two steps. First, bridges with null or duplicate IE records are removed. Second, bridges with clear evidence of maintenance actions are excluded. The aim of the second step is to ensure that the selected bridges represent continuously increasing deterioration that was not interrupted by any maintenance actions. However, since the LTBP database does not provide bridge maintenance records, an indirect approach is followed to exclude bridges with maintenance histories. Specifically, if the time history of the bridge deck condition rating experienced a sudden increase of more than two rating conditions in two consecutive inspections, this bridge is excluded. The reason is that such an increase will not be due to human visual inspection subjectivity but rather a probable major maintenance or reconstruction (Phares et al., 2001). Following the filtration process, 23 bridges were retained for further analysis, where their IE records will be processed to quantify the deck delamination percentage. Note that the decks of the selected bridges all share the same overlay condition (i.e., no deck overlay), which ensures the validity and homogeneity of the selected IE records (ASTM, 2022).

6. DATA PROCESSING

In this step, the IE records of filtered bridges are processed to estimate the delamination percentage for each bridge deck. IE is usually conducted on bridge decks with a grid point spacing range of 0.60–0.90 m to map a condition of deck integrity at each point (Gucunski et al., 2008b). At each grid point, an IE test is conducted producing an IE signal that is recorded. These recorded signals, referred to as the IE record, are then processed to evaluate the extent of delamination. The LTBP database includes both the raw signals and condition maps produced by the NDE company showing the processed interpretation of deck condition. However, the provided condition maps are imperfect and contain numerous artifacts, as will be demonstrated in the Discussion section. Moreover, IE tests were conducted by different companies, which may not use the same techniques/thresholds to interpret the IE raw signals into condition maps. Therefore, to ensure the consistency of the estimated delamination percentage, processing raw IE signals is adopted for this research.

Raw IE signals are first pre-processed to ensure data consistency and to eliminate noise. This preprocessing is achieved by removing the direct current offset by subtracting its mean amplitude from the original signal. The signals are then zero-padded to the nearest power of 2 to ensure good performance when transformed to the frequency domain using the FFT. Finally, the transformed signal is squared and normalized to obtain the normalized spectral amplitude plot. This plot only includes the first 60 kHz values to remove higher frequency values, which usually correspond to noise. The term “IE power spectrum” will be used in the following description to denote the spectrum derived from this preprocessing step.

The processing of the IE signals can be done using the conventional IE data analysis method, which mainly relies on classifying the IE signals based on the peak frequency (i.e., the frequency corresponding to the maximum energy) value only. However, this approach may overlook important energy distribution in areas representing poor or fair conditions, potentially resulting in a less comprehensive assessment. In this study, a more comprehensive method that utilizes both peak frequency and frequency distribution proposed by Sengupta et al. (2021) is adopted. This method provides a more accurate representation of the signal by capturing the full spectrum of energy distribution, thereby offering a deeper insight into the structural condition beyond what peak frequency alone can reveal.

Building on Sengupta et al.’s method, each IE power spectrum signal is classified into one of three classes—good, fair, or poor. This classification is achieved in two steps. **Step 1:** the energy content within three non-overlapping frequency bands is clustered into groups representing good, fair, and poor conditions. This energy content must be calculated for all IE test signals across the available records to ensure a comprehensive analysis. The output of this step is three clusters, each with a unique centroid of relative energy content values in the three bands, which are used in the second step. **Step 2:** This step involves estimating deck delamination for a given bridge deck. In this step, each IE test signal is classified into one of the three clusters based on its relative energy content values and the centroids identified in the previous step. This classification is applied to all IE test signals across the deck, assigning each signal a condition label corresponding to one of the three classes: good, fair, or poor. Finally, the delamination percentage is calculated as the proportion of IE signals classified as poor to the total number of signals, providing a quantitative measure of the deck’s condition. The specific procedures for the two steps are discussed in the following section.

Step 1: Identification of centroids of three classes—good, fair, or poor. The clustering of the IE energy content is achieved by first plotting the histogram of the peak frequency for each IE record. A Gaussian mixture model (GMM) is then used to fit Gaussian curves to the histogram. The Gaussian curve with the largest mixing proportion is selected to represent the thickness resonance frequency (f_{th}). Each IE power spectrum is divided into three distinct frequency bands: Band 1, Band 2, and Band 3. Band 1 captures low-frequency energy below the thickness resonance and is labeled as “poor.” Band 2, representing the thickness resonance frequency dominant in intact decks, is labeled as “good.” Band 3, covering frequencies above the thickness resonance, is labeled as “fair.” The thickness resonance frequency bandwidth (i.e., Band 2) is defined from $(f_{th} - n \cdot \sigma)$ to $(f_{th} + n \cdot \sigma)$, where σ is the standard deviation of the fitted Gaussian curve, and n is the number of standard deviations considered in defining the bands. The bandwidths of Bands 1 and 3 are from 0 to $(f_{th} - n \cdot \sigma)$ and from $(f_{th} + n \cdot \sigma)$ to 60 kHz, respectively. The energy content within each band is calculated, and this process is repeated for all available IE records. When completed, the relative energy percentage in each band for all signals is fed into a K-means clustering algorithm. Running the algorithm with K=3 yields three centroid values for the three different clusters: good, fair, and poor. Although it is possible to adopt this workflow for the selected IE records employed in this study, centroid values from Sengupta et al. (2021) were used because their study employed a larger dataset, including synthetic IE records, to achieve balanced data that accurately represent IE records for decks with varying condition ratings.

Step 2: Assessment of bridge delamination. After the centroids of the three clusters were identified, the clusters were used to estimate the delamination percentage for the selected bridge decks, which had one to three IE records (from one to three inspections). However, to ensure that the modeling data points are independent, only the first available (earliest) IE record for each bridge deck was selected. The reason for that is to avoid any potential underreporting of maintenance activities in subsequent years. For each IE record, delamination estimation was achieved by fitting a GMM model to the peak frequency histogram. Nevertheless, a precise selection process is essential to determine the thickness resonance frequency bandwidth, given the limited number of available bridges after the filtration step (i.e., 23 bridges). Due to the small dataset, the influence of any outlier or poorly processed IE record is magnified, potentially skewing the results significantly. More specifically, multiple dominant frequencies may be present in the frequency histogram. In this case, the estimated bandwidth may not accurately reflect the thickness frequency, but rather peak frequencies associated with delaminations.

To avoid the potential pitfalls described above and ensure more accurate selection of thickness frequency bandwidth, two checks are followed. First, the estimated bandwidth based on the fitted Gaussian curve should overlap with the thickness frequency range calculated by equation (1). This calculated range is obtained by using the available deck thickness and assuming a P-wave velocity range of 3,500–4,500 m/s and a (β) factor of 0.96. Second, the lower limit of the estimated bandwidth should not be less than 5 kHz since, typically, peaks with frequencies less than 5 kHz are caused by the presence of extensive shallow delaminations. Accordingly, if the IE record analysis for one deck did not pass these two checks, this IE record is excluded from the modeling dataset. Histogram examples of both included and excluded IE records are given in Figure 6.1. Also note that the estimated bandwidth used in the checks is chosen as $(f_{th} - \sigma)$ to $(f_{th} + \sigma)$ where the value of n was chosen as 1, similar to Torlapati et al. (2023), and also since this estimated bandwidth better matches the calculated bandwidth from equation (1). For bridge records passing the checks, the relative energy percentage in each band is calculated. Finally, each signal is then classified using the K-nearest neighbor (k-NN) algorithm and Euclidean distance between the test data in terms of the energy contents in each band and the centroid of each class. The delamination percentage is quantified by the proportion of IE signals categorized as "poor" relative to the total number of signals analyzed. The general workflow of the data processing is given in Figure 6.2. Following this workflow yielded 20 IE records, which will be subsequently used to develop the GPR model.

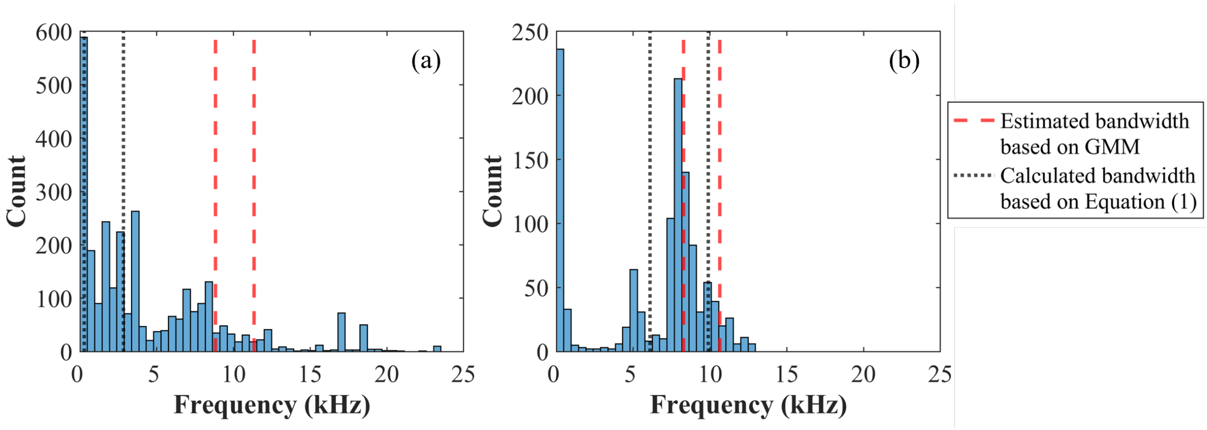

Figure 6.1 Peak histogram examples: (a) record failing both thickness frequency checks since the estimated bandwidth does not overlap with the calculated thickness frequency range and the lower limit of the estimated thickness resonance frequency is less than 5k Hz; (b) record passing both thickness frequency checks.

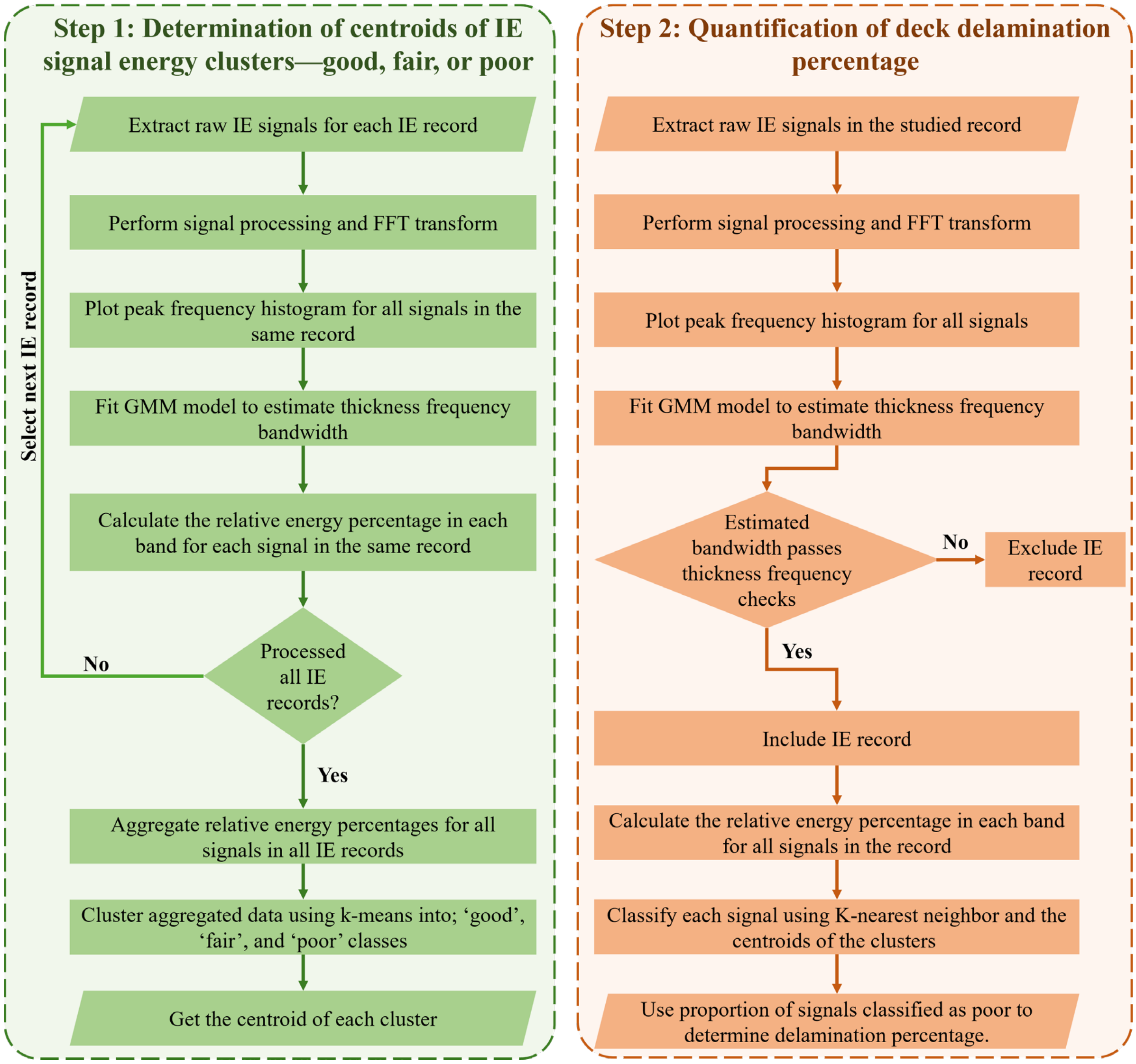

Figure 6.2 Workflow followed in IE signals processing: determination of centroids of IE signal energy clusters—good, fair, or poor (left); quantification of bridge delamination percentage (right)

7. MODELING AND RESULTS

7.1 Explanatory Variables Selection

Bridge deterioration is a complex process that is influenced by many explanatory variables. Different studies have investigated the influence of both structural specifications and environmental conditions on the deterioration rate of roadway and railway bridges (Ghonima et al., 2020; Srikanth & Arockiasamy, 2021). Explanatory variable selection can be based on engineering judgment (Li & Jia, 2021). Based on previous studies and engineering judgment, the explanatory variables shown in Table 1 were selected to be the most influential variables affecting bridge deterioration (Liu & Zhang, 2020; Nguyen & Dinh, 2019).

Table 7.1 Selected explanatory variables for delamination modeling

Explanatory variable	Data source
Structure configuration	
Bridge roadway width - curb to curb	NBI- Item 51
Year built	NBI-Item 27
Skew angle, degrees	NBI-Item 34
Deck thickness	LTBP-design data
Deck top cover	LTBP-design data
Service conditions	
Bridge age	NBI-Item 27
Average daily traffic (ADT)	NBI-Item 29
Average daily truck traffic (ADTT)	NBI-Item 109
Average number of freeze-thaw cycles	LTBP-design data
Deck protection code	NBI-Item 108C

The selected explanatory variables can be divided into two categories. The first category includes structure configuration variables. In this category, bridge roadway width can affect bridge deterioration since the wider the deck, the more it can accommodate traffic loads. Wider decks also have larger exposure areas to environmental effects such as temperature changes and, accordingly, they are more prone to deterioration. The year the bridge was built captures the differences in design, material quality, and construction practices that occur as engineering practices change over time. Considering the deck skew angle, skewed bridges are more prone to non-uniform load distribution, differential deflections, and increased shear forces. Thicker decks generally provide better load distribution, greater thermal stability, and increased durability, all of which help reduce the risk of delamination. Lastly, the deck top cover is the main line of defense that protects the top reinforcement layers from penetrating chlorides, which cause reinforcement corrosion.

The second category of explanatory variables can be referred to as service conditions. In this category, bridge age is one of the main influencing variables and is calculated as the difference between the year built and the inspection year. Bridge age reflects the degradation of materials over time and the length of exposure to other service conditions. Both ADT and ADTT exert a significant impact on bridge decks, with higher traffic volumes, particularly trucks, intensifying deck stresses and accelerating wear, thereby increasing delamination potential. For some bridges, the time history of ADT and ADTT has dramatically changed over time. While cumulative ADT and ADTT values can capture these changes, because of missing records from earlier years these values are averaged over the available time history for each bridge. The annual number of freeze-thaw cycle days can accelerate the delamination process, especially in colder regions. During freeze-thaw cycles, water penetrates concrete, freezes, and expands causing delamination. Besides, in such regions it is common to use deicing salts, which cause corrosion of reinforcement and eventually delamination. Since the number of freeze-thaw cycle days varies from year to year, the average annual number was calculated, following the same approach used for ADT and ADTT. Finally, the deck protection code specifies whether the reinforcement bars are epoxy coated or not. Uncoated bars are more likely to corrode, leading to more delamination.

7.2 Gaussian Process Regression Model

GPR is a flexible non-parametric and data-driven Bayesian approach to regression that maps the input variables to provide a stochastic distribution over functions of the objective output. Prior knowledge is first assumed by specifying the covariance (kernel) function, and posterior over functions are then evaluated given the observed data. GPR is selected to model bridge deterioration for two main reasons. First, GPR can work on small datasets while capturing complex deterioration patterns due to the strong assumptions of the Gaussian process. Second, GPR provides an uncertainty measurement on the predictions without any additional computational cost. Such advantages can help indicate bridges with high prediction uncertainty within the dataset and better inform maintenance decisions.

The gaussian process (GP) is a stochastic process in which every finite subset of those random variables has a multivariate Gaussian distribution. It generalizes the concept of the Gaussian distribution over random variables to continuous functions. The GP is completely defined by its mean $m(\mathbf{x})$ and covariance function $\mathrm{k}(\mathbf{x}, \mathbf{x}')$ (Rasmussen & Williams, 2005) and expressed as:

$$f(x) \sim GP(m(\mathbf{x}), k(\mathbf{x}, \mathbf{x}')) \tag{2}$$

The mean function $m(\mathbf{x})$ represents the expected value of the function $f(\mathbf{x})$ at the input point $\mathbf{x}$ which allows for a greater flexibility in defining prior functions, enhancing the modeling process. The covariance function $\mathrm{k}(\mathbf{x}, \mathbf{x}')$ determines the covariance (or correlation) between any two points in the input space $\mathbf{x}$ and $\mathbf{x}'$. It captures the similarity between input points. The training dataset is expressed as $D = \{(\mathbf{x}_i, y_i)\}_{i=1}^{N}$, where $\mathbf{x}$ denotes the explanatory variables vector and y denotes the delamination percentage. In GP, it is assumed that:

$$y = f(\mathbf{x}) + \epsilon \tag{3}$$

where $f(\mathbf{x})$ is the true function value and ϵ represents an additive noise that follows independent identically distributed Gaussian with zero mean and variance ${\sigma_n}^2$, $\epsilon \sim N(0, {\sigma_n}^2)$.

The GPR process involves the identification of several key parameters, including the mean function, covariance function and its associated hyperparameters, alongside the noise variance. The mean function is usually assumed to be zero for computational simplicity. Several covariance functions have been studied in the literature based on the nature of the problem. However, one common choice is the squared exponential covariance function expressed as:

$$k(\mathbf{x}, \mathbf{x}') = \sigma^2 exp\left(-\frac{1}{2}\left(\frac{\mathbf{x} - \mathbf{x}'}{l}\right)^2\right) \tag{4}$$

where σ^2 and l are free hyperparameters that correspond to signal variance and length scale, respectively. Different covariance functions have different hyperparameters, which can be estimated by maximizing the likelihood function. In the case of a multivariate regression problem, a kernel function with a different length scale for each variable can be used to capture the relative influence between the different variables. In this report, a MATLAB software code was developed to construct the GPR model.

7.3 GPR Hyperparameters Optimization

Hyperparameter optimization is a crucial step that involves tuning the parameters of the Gaussian process model to achieve the best possible performance in terms of predictive accuracy as well as generalization capability. The GPR process typically begins by selecting an expected mean function (often assumed to be zero for simplicity) and a covariance function, which describes the relationship between the explanatory variables and delamination. The hyperparameters in GPR include the covariance function hyperparameters: amplitude standard deviation σ) and length scale (l) as well as noise standard deviation (σ_n). Generally, if enough IE records are available, they can be used to infer information about the expected mean delamination percentage and covariance function. In this case, the different hyperparameters can be optimized by maximizing the likelihood function. However, given the limited data in this study (only 20 data points) and the mix of numeric and categorical explanatory variables, selecting appropriate mean and covariance functions becomes less straightforward. Accordingly, a more robust technique, Bayesian optimization, is employed (Snoek et al., 2012). The Bayesian optimization approach extends the optimization problem to include different possible combinations of the mean and kernel functions. Unlike other optimization algorithms, Bayesian optimization improves the search speed by using past evaluations. This is achieved by calculating a posterior distribution of the objective function based on the likelihood of the data observed so far and an initial assumption about the prior of the function.

The developed GPR model implemented Bayesian optimization using the MATLAB built-in Bayesian optimization algorithm: "fitrgp." The process starts by building a GP proxy model of the objective loss function, which needs to be minimized. The acquisition function then selects the next set of hyperparameters to evaluate by balancing exploration of the search space and exploitation of known areas with promising results. The "expected-improvement-per-second-plus" acquisition function is selected to optimize hyperparameter tuning by evaluating the expected improvement, which measures the expected amount of improvement in the objective function over the current best value. The per-second aspect considers evaluation time and penalizes hyperparameter values that are expected to take a very long time to train. The plus component adjusts the function to prevent overexploitation of local minima by increasing the variance, encouraging exploration of new areas. By iteratively updating the probabilistic GP model and selecting new hyperparameter values, Bayesian optimization progressively converges toward the optimal solution with minimal objective function evaluations, leading to more efficient hyperparameter optimization.

To ensure the reliability of the GPR model and prevent overfitting given the small dataset, cross-validation was employed in the hyperparameter optimization process. With only 20 data points and 10 explanatory variables, the GPR model was trained on 18 data points and tested on two. Bayesian optimization minimized the nine-fold cross-validation loss in nine runs. For each run, 16 points are used for training and two points are left out for validation. Specifically, the objective loss function is expressed as $log(1 + MSE_{CV})$, where MSE_{CV} represents the overall cross-validation loss calculated by averaging the mean squared error (MSE) of the two validation points in each run, and then averaging this value across all nine runs. The MATLAB built-in Bayesian optimization algorithm searches for the optimal mean function from four candidates: "constant," "none," "linear," and "pureQuadratic." Additionally, it identifies the best kernel function and its corresponding hyperparameters from a set of 10 options: "ardexponential," "ardmatern32," "ardmatern52," "ardrationalquadratic," "ardsquaredexponential," "exponential," "matern32," "matern52," "rationalquadratic," and "squaredexponential," The algorithm further optimizes the noise variance and determines if data standardization is necessary.

7.4 Results

The results of the hyperparameter optimization for the GPR model are first discussed to highlight the effectiveness of Bayesian optimization in improving predictive accuracy of the GRP model. The runs of objective function evaluations in the hyperparameter optimization were increased from the default value of 30 to 60 to ensure convergence to an optimized solution (Figure 7.1). The final results of hyperparameter optimization are as follows: standardized data, a noise variance of 7.58%, a zero-mean function, an amplitude standard deviation of 33.75%, and an ARD-squared exponential kernel. These parameters together optimized the model's performance. The ARD-squared exponential is a variant of the squared exponential kernel, where ARD stands for automatic relevance determination (Neal, 1996), allowing each variable to have a unique length scale. The selection of the squared exponential kernel is particularly appropriate here as it implies that bridges with similar characteristics will exhibit similar delamination patterns, reflecting the smooth and continuous nature of the underlying physical process.

The final optimized GPR model demonstrated strong predictive performance, as demonstrated by the cross-validation results in Figure 7.2(a). In this figure, the predicted delamination percentages generally align well with the actual delamination percentages across most runs, indicating that the model's hyperparameters have been effectively optimized despite the limited data (16 data points for training per run). In runs such as 3 and 4, the predictions closely match the actual values, demonstrating the model's accuracy. However, discrepancies are evident in run 7, where the predicted values are noticeably higher than the actual, suggesting the model struggles with cases that differ significantly from the training data. Across all nine runs, the model achieved an average RMSE of 11.45%, with six of those runs having an RMSE below 10%, as shown in Figure 7.2(b). The predicted standard deviations [Figure 7.2(a)] remain small in most runs, indicating a fair level of confidence, though slight increases in uncertainty are observed in runs 7 and 8. This increased uncertainty is due to the larger differences of explanatory variables between the validation data and training data within these two runs. Finally, the optimized hyperparameters were used to train the model on the full dataset (18 data points). The model was then tested on two previously unseen data points, which were not part of the training or cross-validation process. The model achieved an average RMSE of 10.70% for these two points, with prediction standard deviations of 10.34% and 11.46%, as shown in Figure 7.3. The results demonstrate the model's robustness and its ability to generalize to new data while maintaining reasonable accuracy.

One approach to show the relative importance of the selected explanatory variables is to plot the log of length scale for each variable, as shown in Figure 7.4. In this case, variables with smaller length scales have a greater influence on the delamination percentage, as the model responds more sensitively to changes in these variables. Figure 7.4 highlights that the number of freeze-thaw cycles is the most significant factor affecting bridge deck delamination. This finding is consistent with the ACI Committee 116 report, which identifies freeze-thaw cycles as a primary cause of delamination (ACI Committee 116R-00, 2003). Deck thickness also has a notable impact, as thicker decks generally provide better resistance to environmental stresses. Skew angle, while less critical, still contributes to vulnerability, as larger angles can lead to stress concentrations and cracking. A survey conducted among New York State DOT regional bridge maintenance engineers indicated that 96% (22 out of 23) of the participants viewed skewed bridges to have higher maintenance needs (Diaz Arancibia et al., 2020). Deck protection code and top cover show comparable influences, as both play a role in reducing the exposure of reinforcing steel to corrosive elements, thus mitigating corrosion and reducing the risk of delamination (Cady & Weyers, 1984; Pincheira et al., 2015). Traffic-related variables, such as ADTT and ADT, moderately affect delamination, as increased traffic volumes accelerate deterioration. In contrast, both the age of the bridge and the year it was built appear to have minimal impact, with bridge roadway width identified as the least important variable in determining delamination.

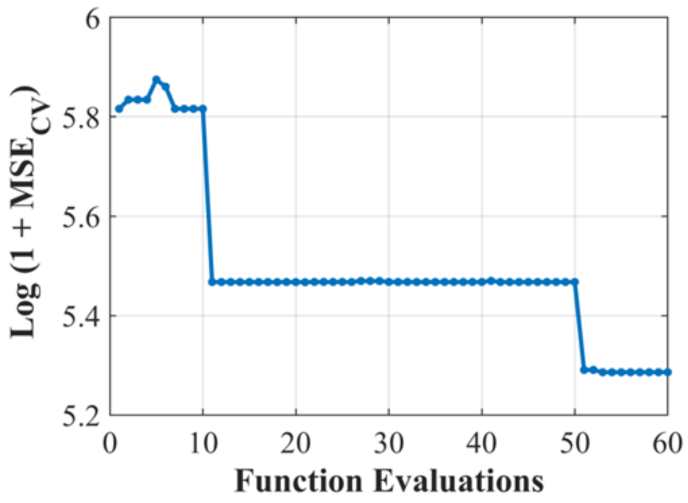

Figure 7.1 Evolution of objective function with the number of evaluations

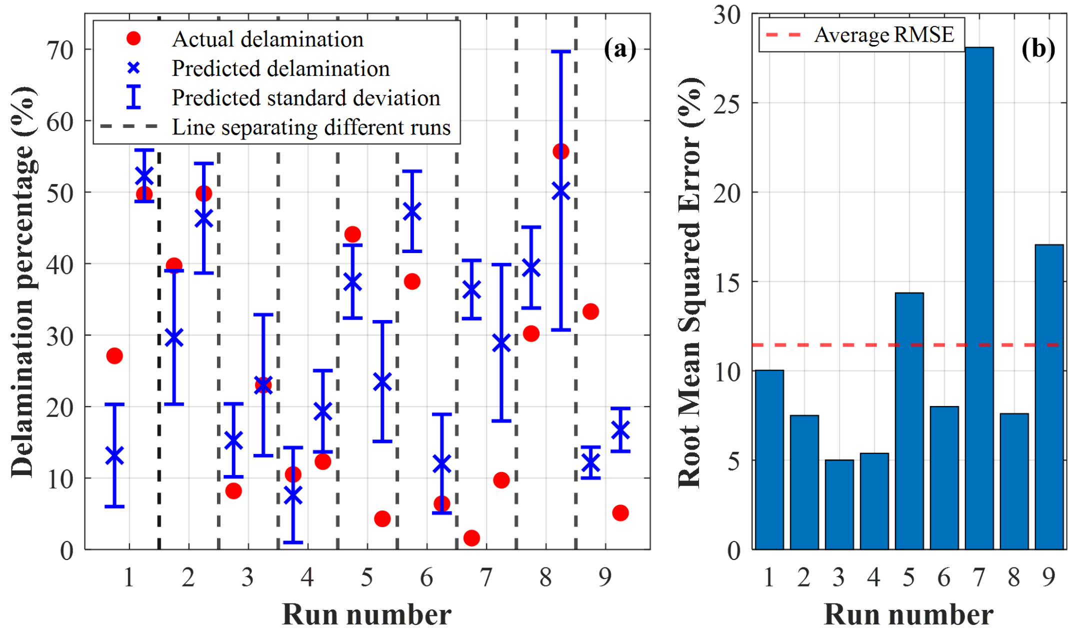

Figure 7.2 GPR predictions cross-validation results: (a) cross-validation predictions, and (b) cross-validation RMSE results

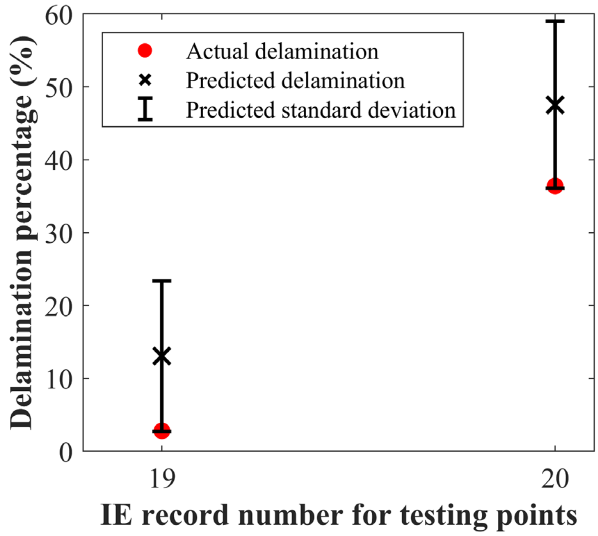

Figure 7.3 GPR prediction results for testing data

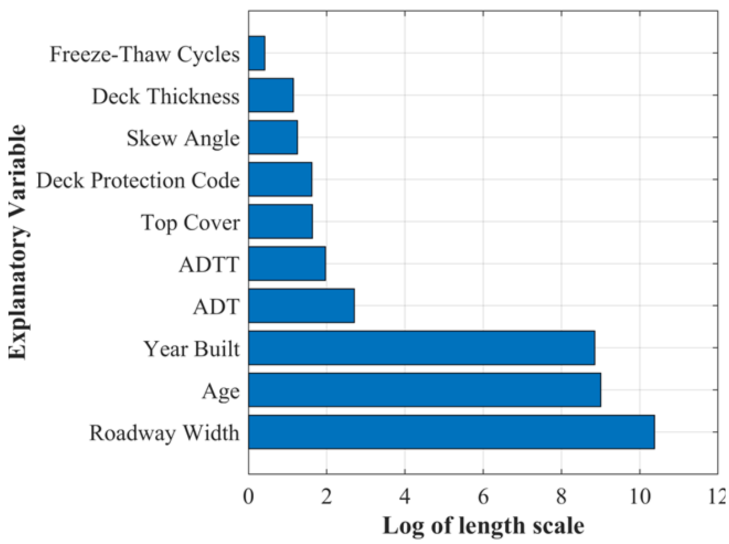

Figure 7.4 Relative importance of variables expressed by the log of length scale

8. DISCUSSION

This report demonstrates the application of GPR to bridge NDE data for developing quantitative predictions of deterioration. An important implication of this modeling approach is its potential use in strategically allocating NDE inspections to enhance model predictions, particularly through uncertainty prediction. However, the analysis and model development were not fully optimized due to several data limitations of NDE data available in the LTBP database. The effectiveness of leveraging NDE data provided in the LTBP database can be significantly improved by addressing these limitations and incorporating additional crucial non-NDE data that are currently missing. By filling these gaps, the overall quality of the dataset would be enhanced, leading to better predictive accuracy and more reliable bridge condition assessments, ultimately improving decision-making in bridge management.

The developed GPR model offers two key advantages in predicting deck delamination, particularly for bridges without IE records. First, it enables accurate delamination predictions for bridges with characteristics similar to those used in training, providing actionable insights without the need for immediate testing. Second, the model optimizes the selection of bridges for NDE testing by identifying those with high prediction uncertainty. By incorporating uncertainty estimation for each prediction, the GPR model prioritizes bridges with the highest uncertainty for testing, ensuring that resources are allocated efficiently. This approach not only improves the accuracy of future predictions by focusing on bridges with the greatest uncertainty, but it also enhances overall bridge management by targeting the most uncertain structures for inspection, ensuring resources are deployed where they are most needed.

To visually illustrate the two main advantages of the GPR model, a schematic diagram of a GPR model has been developed to represent the relationship between the explanatory variables vector and the predicted delamination percentage. In Figure 8.1(a), the testing points have characteristics similar to those of the training data, resulting in low prediction uncertainty. In this case, the predicted delamination values can be confidently used to guide maintenance decisions, demonstrating the model's first advantage. In Figure 8.1(b), the three testing points, shown with varying levels of uncertainty, differ significantly from the training data. This leads to higher uncertainty in predictions, especially for Bridges 1 and 2, which show the largest uncertainty. In this case, considering available financial resources, Bridges 1 and 2 should be prioritized for NDE scheduling to refine future predictions and optimize resource allocation.

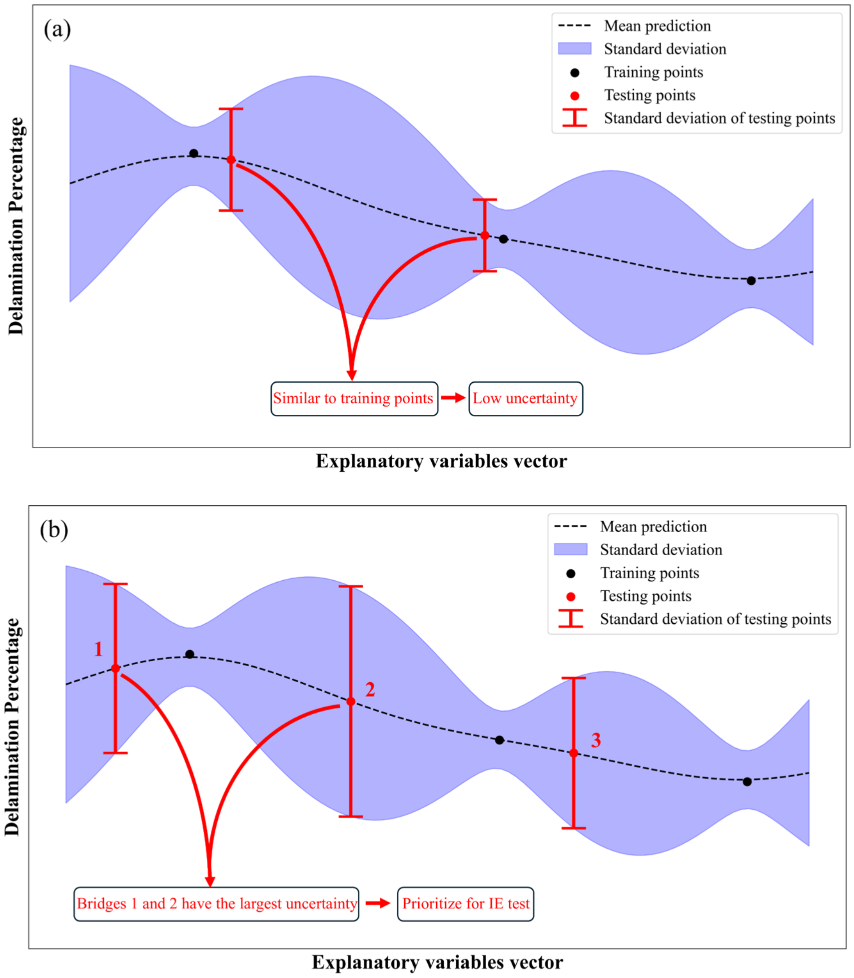

Figure 8.1 Main advantages of the GPR model: (a) predicting delamination percentage for bridges similar to those in the training data; (b) identifying bridges with high uncertainty for prioritized IE testing and scheduling.

This approach of employing GPR for future IE test scheduling can be employed for any NDE output. Accordingly, this can be utilized to establish an NDE inspection planning framework. In this framework, inventory bridges are evaluated using the existing GPR model to quantify prediction uncertainty for each bridge. Bridges with high prediction uncertainty, along with available resources and funds, are prioritized for the upcoming NDE tests. After the NDE tests are conducted, the deterioration estimates are used to update the NDE records database. This updated database is then used to fit a new GPR model, with model parameters optimized via Bayesian optimization. This iterative process continues until a sufficient number of NDE records is available, at which point the model will deliver strong predictive performance with acceptable uncertainty. This proposed framework is shown in Figure 8.2.

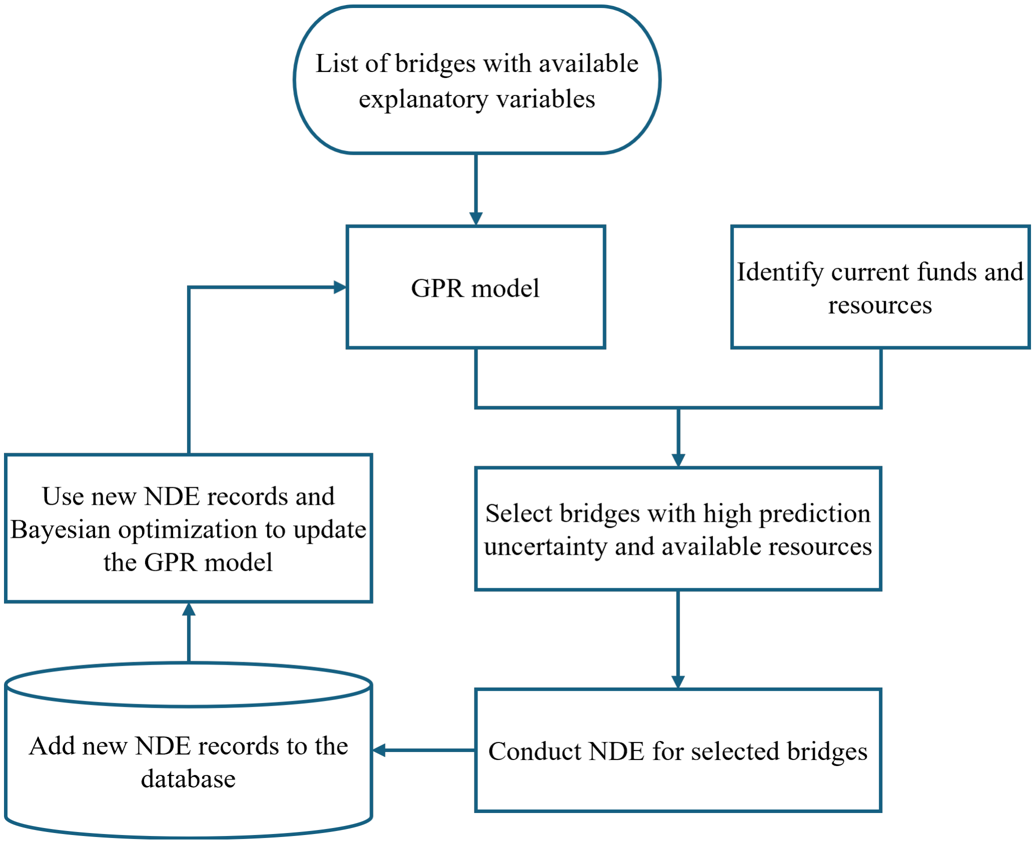

Figure 8.2 Proposed NDE inspection planning framework

Although the developed GPR model has delivered promising results, its predictive accuracy can be further improved by addressing key limitations in the NDE data available in the LTBP database. A more comprehensive and complete dataset would strengthen the model's ability to generalize across diverse bridge conditions. A thorough investigation of the NDE data provided in the LTBP database has revealed several critical limitations that, if addressed, could significantly enhance the model's predictive capabilities and overall performance. These limitations include:

- A very limited number of bridges with NDE records (38 bridges) exist on the LTBP when compared with the number of bridges in the inventory (620,700 bridges).
- Previously detected delaminated areas were sometimes not identified in subsequent inspections, likely due to variations in test operators and differences in scanned area dimensions across different years.
- There was no standardized format for presenting the NDE results. Some NDE maps were displayed in colored condition maps to represent poor to sound conditions, while others showed the actual return frequency magnitude values.
- Deck information, including concrete specifications, thickness, and reinforcement details, is crucial for interpreting NDE data, yet only 26 bridges have these data available.
- For some bridges, deck specifications such as skew angle, do not match between the NBI data and the LTBP design data.
- For NDE condition maps, some have missing areas due to errors and terminations in the automated scanning process, as shown in Figure 8.3.
- For some bridges, particularly those with automated scans, irregularities in test point locations were evident, including missing and overlapping areas, as shown in Figure 8.4.
- Finally, the available NDE data are geographically restricted to the eastern U.S., resulting in a dataset that lacks diversity in environmental conditions.

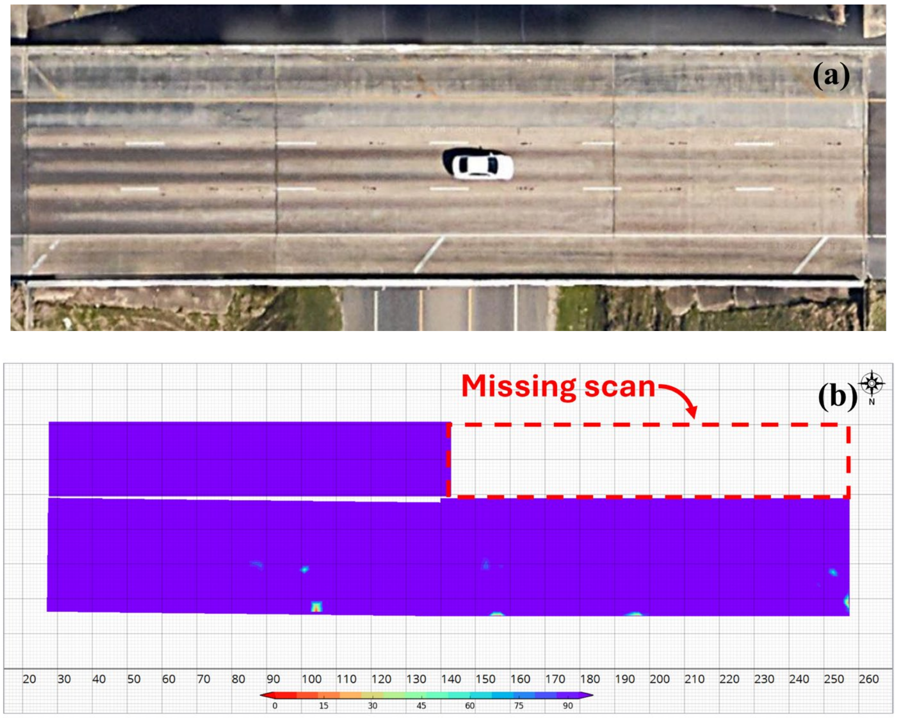

Figure 8.3 Example of NDE condition map with missing scans: (a) actual bridge image from Google Maps; (b) ER map from LTBP showing missing scan areas caused by automated scan self-termination (LTBP).

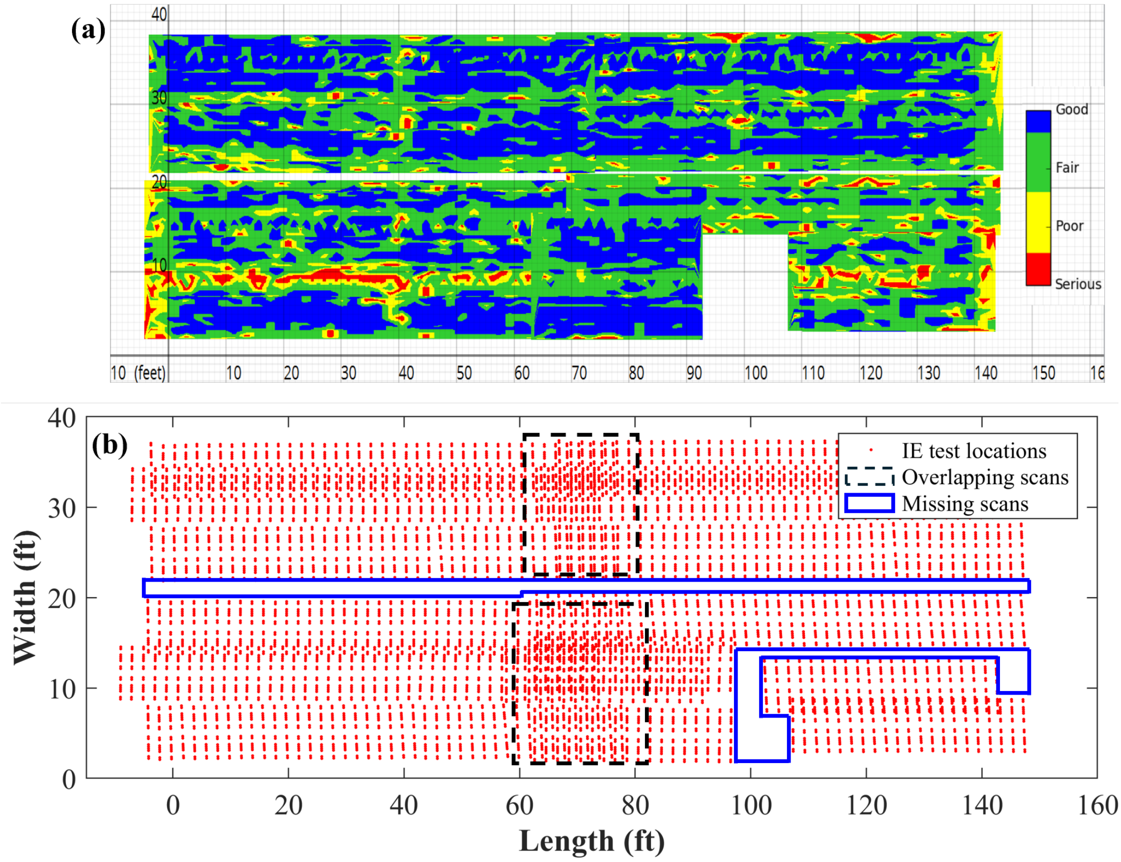

Figure 8.4 Example of deck IE test: (a) processed IE condition map; (b) corresponding IE test locations with missing and overlapping scan areas (LTBP).

The aforementioned limitations can be effectively addressed by implementing the following actions:

- Increase the number of bridges with NDE data provided.
- Standardize aspects of the NDE data collection, data processing, and reporting process to allow data from different inspection companies to be used collectively with ease.
- Include detailed information about the NDE test equipment, such as technical specifications, calibration status, and environmental conditions (e.g., temperature, humidity, wind speed).
- Document any interruptions or terminations during automated scans, specifying the underlying causes (e.g., equipment malfunction, positioning errors, or environmental factors), the affected scan areas, and whether these sections were omitted or re-scanned, potentially resulting in overlapping data. Include a description of the corrective actions taken to ensure transparency, consistency, and completeness of the dataset.
- Conduct a quality check on all NDE records to ensure consistency in scanned areas and to identify any overlapping or missing scans.

Finally, several critical gaps related to other non-NDE data in the LTBP bridge database have been identified, and addressing these gaps would significantly enhance the filtration and deterioration modeling processes. Specifically, while maintenance data are included in the LTBP Program protocols, they are notably absent from the database. These data are vital for accurately tracking and understanding bridge deterioration, particularly since each state DOT follows distinct maintenance and rehabilitation policies. Additionally, the application of deicing and anti-freezing chemicals, though cost-effective, contributes to bridge deck degradation and reinforcement corrosion. Collecting detailed data on their use could yield valuable insights into their long-term effects and cost-effectiveness. Furthermore, construction practices and design data—such as soil compaction techniques, concrete placement, curing methods, welding, and fastening—are essential for determining bridge service life. However, design data are available for only a limited number of bridges, with just 1,580 out of 620,669 bridges having design data, and only 26 bridges having both NDE and design data. Addressing these data gaps is crucial for improving the accuracy and reliability of bridge deterioration models.

9. CONCLUSIONS

This report introduces a novel concept for leveraging limited NDE data, which is often underutilized. Currently, NDE data are only used to evaluate the condition for a specific bridge being tested. The proposed GPR model offers a new way to collectively use the data across different bridges to provide two valuable advantages. First, it enables accurate delamination predictions for untested bridge decks with characteristics similar to the training data, offering actionable insights without the need for immediate testing. Second, it optimizes NDE testing by prioritizing bridges with high prediction uncertainty, ensuring that resources are allocated efficiently. This approach not only improves the accuracy of future predictions by focusing on bridges with the greatest uncertainty, but it also enhances overall bridge management by targeting the most uncertain structures for inspection, ensuring resources are deployed where they are most needed.

This concept was demonstrated using existing IE test records from the LTBP database to predict future delamination percentages, accompanied by associated uncertainty measures. When tested on bridges with similar environmental conditions and characteristics, the model achieved an average RMSE of 11.45% for cross-validation data and 10.70% for testing data. Analysis of the model revealed that the number of freeze-thaw cycles is the most critical factor influencing bridge deck delamination, followed by deck thickness. Finally, this report identifies the current limitations in the NDE data available in the LTBP database and suggests actions to address them, leading to improvements in future data collection. Additionally, several critical gaps related to non-NDE data have been identified to enhance the deterioration modeling processes. Further exploration of this approach is recommended to enhance the accuracy and reliability of bridge deterioration predictions once more data become available.

10. REFERENCES

ACI Committee 116R-00. (2003). “Cement and concrete terminology.” In *Manual of Concrete Practice* (Part 1). American Concrete Institute.

Althaqafi, E., & Chou, E. (2022). “Developing bridge deterioration models using an artificial neural network.” *Infrastructures*, *7*(8). https://doi.org/10.3390/infrastructures7080101

ASTM. (2022). “Standard test method for measuring the P-wave speed and the thickness of concrete plates using the impact-echo method (ASTM C1383-15).” ASTM International. Retrieved October 29, 2024, from https://www.astm.org/c1383-15r22.html

Cady, P. D., & Weyers, R. E. (1984). “Deterioration rates of concrete bridge decks.” *Journal of Transportation Engineering*, *110*(1), 34–44. https://doi.org/10.1061/(ASCE)0733-947X(1984)110:1(34)

Caltrans Division of Research, Innovation, and System Information. (2020). “Bridge Deterioration Models and Rates (Preliminary Investigation PI-0274).” California Department of Transportation. Retrieved from https://dot.ca.gov/-/media/dot-media/programs/research-innovation-system-information/documents/preliminary-investigations/pi-0274-a11y.pdf

Concrete New Zealand Incorporated. (2021). *Guide to Minimising the Risk of Delamination in Concrete* (ISBN: 978-0-908956-83-8). Concrete New Zealand. Retrieved from https://concretenz.org.nz/news/575864/Minimise-the-Risk-of-Delamination-in-Concrete.htm

Dhada, M., Hadjidemetriou, G. M., & Parlikad, A. K. (2020). “Predicting bridge elements deterioration using collaborative Gaussian process regression.” *IFAC-PapersOnLine*, *53*(3), 348–353. https://doi.org/10.1016/j.ifacol.2020.11.056

Diaz Arancibia, M., Rugar, L., & Okumus, P. (2020). “Role of skew on bridge performance.” *Transportation Research Record: Journal of the Transportation Research Board*, *2674*(5), 282–292. https://doi.org/10.1177/0361198120914617

Federal Highway Administration. (2023). *2023 - Bridge Condition by Highway System - National Bridge Inventory - Bridge Inspection - Safety Inspection - Bridges & Structures*. Retrieved October 29, 2024, from https://www.fhwa.dot.gov/bridge/nbi/no10/condition23.cfm

Federal Highway Administration. (2024). *Performance History - LTBP InfoBridge*. U.S. Department of Transportation. Retrieved October 29, 2024, from https://infobridge.fhwa.dot.gov/

Fu, G., & Devaraj, D. (2008). “Methodology of homogeneous and non-homogeneous Markov chains for modeling bridge element deterioration” (Final Report). Wayne State University, Center for Advanced Bridge Engineering. Michigan Department of Transportation. Retrieved from https://rosap.ntl.bts.gov/view/dot/18196

Ghonima, O., Anderson, J. C., Schumacher, T., & Unnikrishnan, A. (2020). “Performance of US concrete highway bridge decks characterized by random parameters binary logistic regression.” *ASCE-ASME Journal of Risk and Uncertainty in Engineering Systems, Part A: Civil Engineering*, *6*(1). https://doi.org/10.1061/AJRUA6.0001031

Gucunski, N., Imani, A., Romero, F., Nazarian, S., Yuan, D., Wiggenhauser, H., Shokouhi, P., Taffe, A., & Kutrubes, D. (2012). “Nondestructive testing to identify concrete bridge deck deterioration.” *Transportation Research Board*. https://doi.org/10.17226/22771

Gucunski, N., Maher, A., Basily, B. B., & La, H. M. (2013). “Robotic platform RABIT for condition assessment of concrete bridge decks using multiple NDE technologies.” *HDKBR Info Mag*, *3*, 4.

Gucunski, N., Pailes, B., Kim, J., Azari, H., & Dinh, K. (2017). “Capture and quantification of deterioration progression in concrete bridge decks through periodical NDE surveys.” *Journal of Infrastructure Systems*, *23*(1). https://doi.org/10.1061/(asce)is.1943-555x.0000321

Gucunski, N., Slabaugh, G., Wang, Z., Fang, T., & Maher, A. (2008). “Impact echo data from bridge deck testing.” *Transportation Research Record: Journal of the Transportation Research Board*, *2050*(1), 111–121. https://doi.org/10.3141/2050-11

Huang, Y.-H. (2010). “Artificial neural network model of bridge deterioration.” *Journal of Performance of Constructed Facilities*, *24*(6), 597–602. https://doi.org/10.1061/(ASCE)CF.1943-5509.0000124

Ilbeigi, M., & Ebrahimi Meimand, M. (2020). “Statistical forecasting of bridge deterioration conditions.” *Journal of Performance of Constructed Facilities*, *34*(1). https://doi.org/10.1061/(asce)cf.1943-5509.0001347

Kim, Y. J., & Yoon, D. K. (2009). “Identifying critical sources of bridge deterioration in cold regions through the constructed bridges in North Dakota.” *Journal of Bridge Engineering*, *15*(5), 542–552. https://doi.org/10.1061/(ASCE)BE.1943-5592.0000087

Lee, Y. H., & Oh, T. (2016). “The measurement of P-, S-, and R-wave velocities to evaluate the condition of reinforced and prestressed concrete slabs.” *Advances in Materials Science and Engineering*, *2016*, 1–14. https://doi.org/10.1155/2016/1548215

Li, M., & Jia, G. (2021). “Age, state, and environment dependent non-homogeneous stochastic model for improved bridge deterioration prediction.” In *Bridge Maintenance, Safety, Management, Life-Cycle Sustainability and Innovations* (pp. 2766–2773). CRC Press. https://doi.org/10.1201/9780429279119-377

Liu, H., & Zhang, Y. (2020). “Bridge condition rating data modeling using deep learning algorithm.” *Structure and Infrastructure Engineering*, *16*(10), 1447–1460. https://doi.org/10.1080/15732479.2020.1712610

Mauch, M., & Madanat, S. (2001). “Semiparametric hazard rate models of reinforced concrete bridge deck deterioration.” *Journal of Infrastructure Systems*, *7*(2), 49–57. https://doi.org/10.1061/(ASCE)1076-0342(2001)7:2(49)

Michigan Department of Transportation (MDOT). (2021). *Bridge management and scoping*. Retrieved October 29, 2024, from https://www.michigan.gov/mdot/programs/bridges-and-structures/structure-preservation

Morcous, G., & Lounis, Z. (2007). “Probabilistic and mechanistic deterioration models for bridge management.” In *Congress on Computing in Civil Engineering, Proceedings* (pp. 364–373). https://doi.org/10.1061/40937(261)45

Morcous, G., Lounis, Z., & Cho, Y. (2010). “An integrated system for bridge management using probabilistic and mechanistic deterioration models: Application to bridge decks.” *KSCE Journal of Civil Engineering*, *14*, 527–537. https://doi.org/10.1007/s12205-010-0527-4

Morcous, G., Rivard, H., & Hanna, A. M. (2002). “Modeling bridge deterioration using case-based reasoning.” *Journal of Infrastructure Systems*, *8*(3), 86–95. https://doi.org/10.1061/(ASCE)1076-0342(2002)8:3(86)

Neal, R. M. (1996). *Bayesian Learning for Neural Networks* (Vol. 118). Springer Science+Business Media. https://doi.org/10.1007/978-1-4612-0745-0

Nguyen, T. T., & Dinh, K. (2019). “Prediction of bridge deck condition rating based on artificial neural networks.” *Journal of Science and Technology in Civil Engineering (STCE) - NUCE*, *13*(3), 15–25. https://doi.org/10.31814/stce.nuce2019-13(3)-02

Nickless, K., & Atadero, R. A. (2018). “Mechanistic deterioration modeling for bridge design and management.” *Journal of Bridge Engineering*, *23*(5), 04018018. https://doi.org/10.1061/(asce)be.1943-5592.0001223

Phares, B. M., Graybeal, B. A., Rolander, D. D., Moore, M. E., & Washer, G. A. (2001). “Reliability and accuracy of routine inspection of highway bridges.” *Transportation Research Record: Journal of the Transportation Research Board*, *1749*(1), 82–92. https://doi.org/10.3141/1749-13

Pincheira, J. A., Aramayo, A., Fratta, D., & Kim, K.-S. (2015). “Corrosion performance of epoxy-coated bars in four bridge decks subjected to deicing salts: 30-year perspective.” *Journal of Performance of Constructed Facilities*, *29*(4), 04014097. https://doi.org/10.1061/(ASCE)CF.1943-5509.0000592

Rasmussen, C. E., & Williams, C. K. I. (2005). *Gaussian Processes for Machine Learning*. The MIT Press. https://doi.org/10.7551/mitpress/3206.001.0001

Sengupta, A., Ilgin Guler, S., & Shokouhi, P. (2021). “Interpreting impact echo data to predict condition rating of concrete bridge decks: A machine-learning approach.” *Journal of Bridge Engineering*, *26*(8). https://doi.org/10.1061/(ASCE)BE.1943-5592.0001744

Snoek, J., Larochelle, H., & Adams, R. (2012). “Practical Bayesian optimization of machine learning algorithms.” In *Neural Information Processing Systems* (pp. 2951–2959).

Sobanjo, J. (1997). “A neural network approach to modeling bridge deterioration.” In *4th Congress on Computing in Civil Engineering, ASCE* (pp. 623–626).

Srikanth, I., & Arockiasamy, M. (2020). “Deterioration models for prediction of remaining useful life of timber and concrete bridges: A review.” *Journal of Traffic and Transportation Engineering (English Edition)*, *7*(2), 152–173. https://doi.org/10.1016/j.jtte.2019.09.005

Srikanth, I., & Arockiasamy, M. (2021). “Remaining service life prediction of aging concrete bridges based on multiple relevant explanatory variables.” *Practice Periodical on Structural Design and Construction*, *26*(4), 04021036. https://doi.org/10.1061/(ASCE)SC.1943-5576.0000604

Taylor, B. R., Qiao, Y., Bowman, M. D., & Labi, S. (2016). *The Economic Impact of Implementing Nondestructive Testing of Reinforced Concrete Bridge Decks in Indiana* (Joint Transportation Research Program Publication No. FHWA/IN/JTRP-2016/20). Purdue University. https://doi.org/10.5703/1288284316343

Tokdemir, O. B., Ayvalik, C., & Mohammadi, J. (2000). “Prediction of highway bridge performance by artificial neural networks and genetic algorithms.” In *Proceedings of the 17th International Symposium on Automation and Robotics in Construction (ISARC)*. https://doi.org/10.22260/ISARC2000/0066

Torlapati, R., Azari, H., & Shokouhi, P. (2023). “Classification of impact echo signals using explainable deep learning and transfer learning approaches.” *Transportation Research Record: Journal of the Transportation Research Board*, *2677*(9), 464–477. https://doi.org/10.1177/03611981231159404

Winn, E. (2011). “Artificial neural network models for the prediction of bridge deck condition ratings” (master’s thesis). Michigan State University.

Winn, E. K., & Burgueño, R. (2013). *Development and validation of deterioration models for concrete bridge decks: Phase 1: Artificial intelligence models and bridge management system* (Report No. CEE-RR-2013/01). Department of Civil and Environmental Engineering, Michigan State University.